In the Proceedings of the 1997 American Controls Conference in
Albuquerque, NM, June 3-6 1997.

Measurements for the PES Pareto Method of Identifying Contributors to Disk Drive Servo System Errors

Terril Hurst
Hewlett-Packard Laboratories
1501 Page Mill Road, M/S 2U-10
Palo Alto, CA 94304
E-mail: terril@hpl.hp.com

Daniel Abramovitch
Hewlett-Packard Laboratories
1501 Page Mill Road, M/S 2U-10
Palo Alto, CA 94304
E-mail: danny@hpl.hp.com

Dick Henze
Hewlett-Packard Laboratories
1501 Page Mill Road, M/S 2U-10
Palo Alto, CA 94304
E-mail: Dick_Henze@hpl.hp.com

Abstract– This is the second in a series of three papers describing a method of allocating the uncertainty in the Position Error Signal (PES) of a magnetic disk drive servo system among its constitutive components ("noises"). Once identified and ranked, the most critical noises can be attacked first, either by finding ways of reducing them or by altering system components to be less sensitive to them. The method requires the measurement of frequency response functions and output power spectra of each servo system element. Each input noise spectrum can then be inferred and applied to the closed loop model to determine its effect on the PES uncertainty. The current paper describes the techniques and measurements that were obtained as part of the PES Pareto Method.

1. Measurements for the PES Pareto Method

In a companion paper [1], a method is presented for separating the contributions of various sources of uncertainty ("noises") in the Position Error Signal (PES) of the track–follow servo in a disk drive. This method requires the construction, from measurements or design models, of component filters and output power spectra; these filters and spectra are then used to compute input noise spectra. The noise spectra are then fed individually through the closed loop model to determine their individual contribution to PES uncertainty [2].

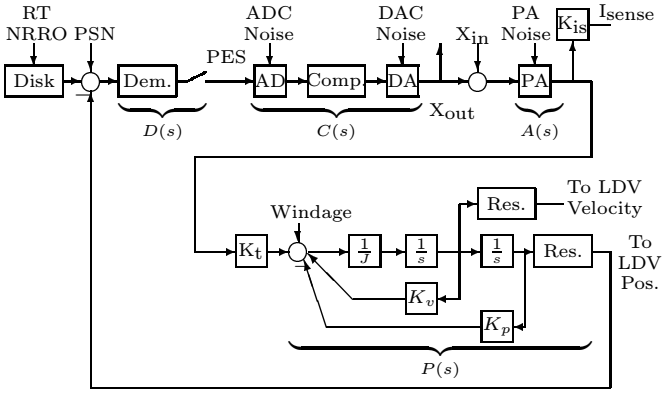

Figure 1: Generalized view of track following model.

1.1 Available Measurement Points. Figure 1 illustrates the disk drive track–follow servo system, including the measurement points (shown in bold font) which are available for gathering the required data. These measurement points are (1) PES, the servo demodulator output; (2) X_{in}, a loop stimulus point; (3) X_{out}, the command current into the actuator power amplifier; (4) I_{sense}, a measurement of actuator coil current; and (5) LDV velocity, measuring the head's radial movement (LDV position was also available, but is better suited in this case for low–frequency measurements—i.e., below 20 Hz). The LDV's velocity output was integrated to obtain displacement information.

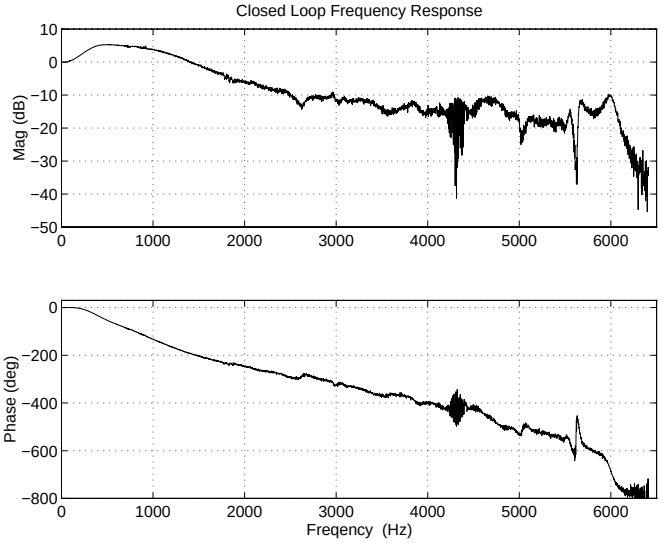

Figure 2: Measured Closed Loop Transfer Function.

All frequency response function (FRF) and power spectral density (PSD) data must be taken over the the same bandwidth and with the same resolution (10-6410 Hz and 2 Hz, respectively, in this case).

1.2 Instrumentation and Data Processing. In addition to the device under test (3.5–inch disk drive) and associated control software and systems, the primary measurement toolset included a laser Doppler vibrometer (LDV, from Polytec), a 5-channel digital signal analyzer (HP 3567A), a digital storage oscilloscope (HP 54720D), and Matlab software running on a workstation.

2. Frequency Response Functions

Figure 2 illustrates the closed loop transfer function which was obtained by measuring the swept–sine response, $Xout/Xin$. (The spike near 4400 Hz indicates the Nyquist frequency.) The open loop transfer function can then be calculated from the closed loop measurement. The compensator transfer function, $Xout/PES$ is shown in Figure 3, and the "mechanics" transfer function, $LDV/Torque$ (where Torque has been calculated by multiplying Isense by Kt), is shown in

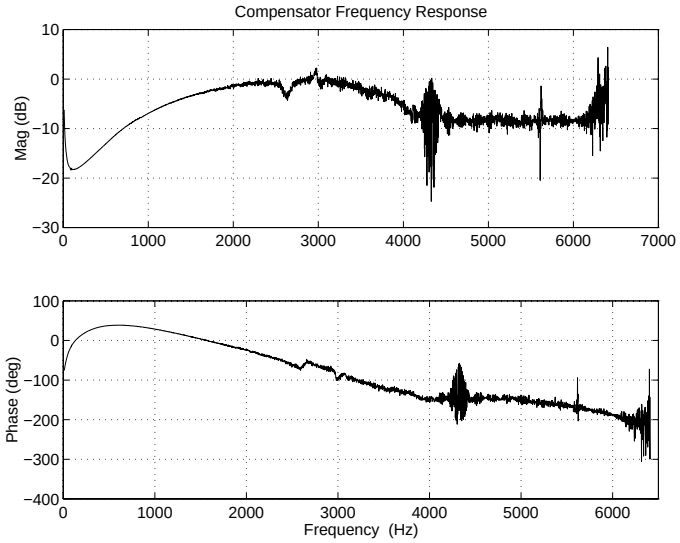

Figure 3: Track–Follow Compensator Transfer Function

Figure 4.

Smoothed versions of all three transfer functions were created for more convenient computation throughout the PES Pareto method. Since the input and output of each block is a power spectrum, it is actually the squared magnitude of each transfer function block (or its inverse) that is used in all computations.

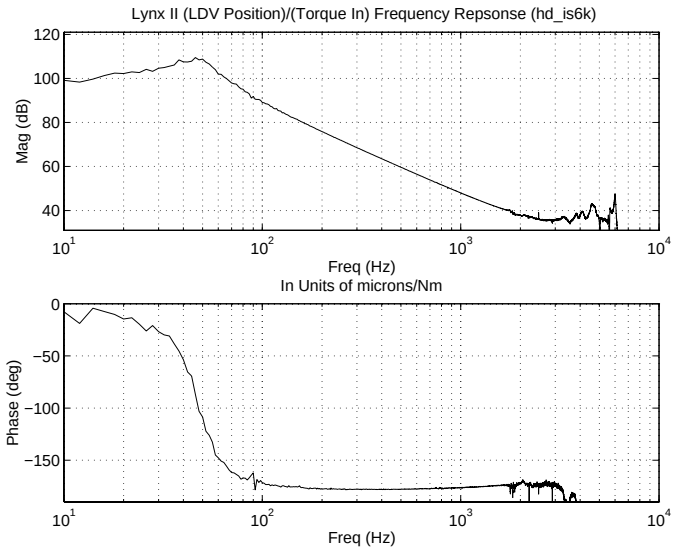

Figure 4: Actuator/Mechanics Transfer Function.

3. Power Spectra

The following power spectra were obtained from each of the measurement points illustrated in Figure 1, with system parameters being varied in order to assess the system's sensitivity to each noise source. We present these power spectra in the order suggested by the system diagram, beginning with PES and ending with estimates of Position Sensing Noise (PSN). The analysis of PSN is presented last, because it relies on a different type of measurement and analysis than the other noises.

Detailed discussion of how this data is used in the PES Pareto method is given in [2]. The data presented here has been filtered to remove synchronous spectral lines, since we were interested primarily in the PES broadband baseline effects.

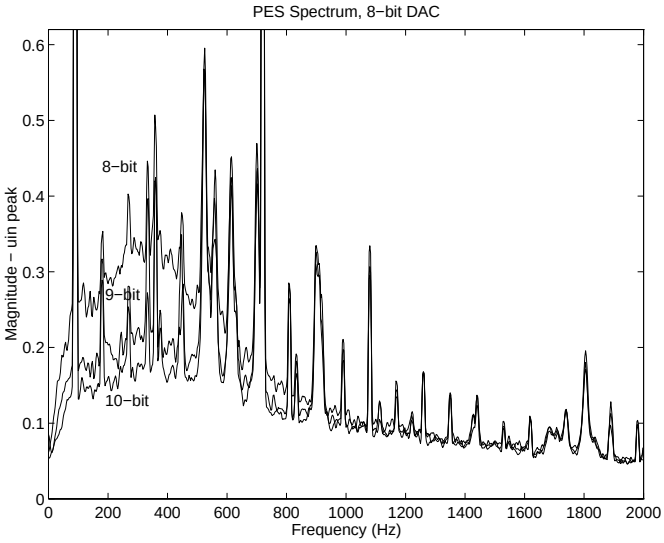

Figure 5: Effect of DAC Resolution on PES.

3.1 DAC and ADC Resolution. One suggested source of PES uncertainty is the finite resolution of the digital–to–analog (DAC) and analog–to–digital (ADC) converters on either side of the compensator. The starting point for determining this uncertainty was to successively mask off bits of each converter and observe changes in the PES power spectrum. This was accomplished by colleagues at HP's Disk Memory Division (using a bandwidth of 2000 Hz rather than the 6400 Hz bandwidth which we used in our measurements). Figure 5 illustrates the sensitivity of PES to DAC resolution, and Figure 6 shows the comparitively smaller effect of reducing ADC resolution. (*Note:* As mentioned in our previous paper [1], we concentrated on the PES baseline; hence, sharp spectral lines due to synchronous sources and bearing cage orders have been eliminated.) These spectra were later subtracted from each other in order to isolate quantization noise [2].

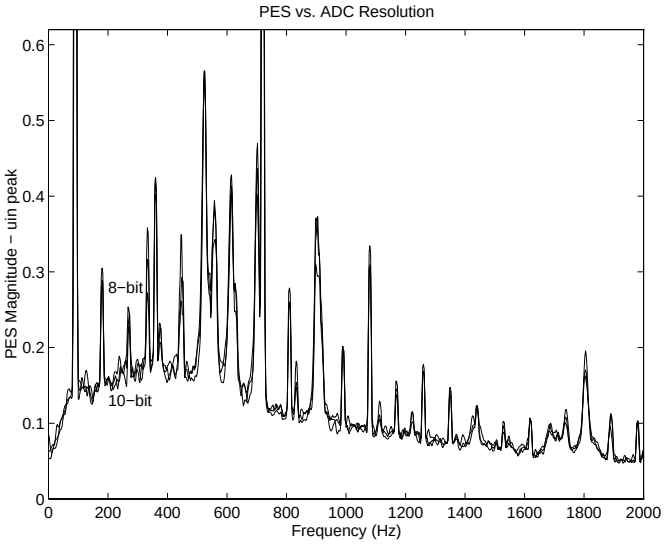

Figure 6: Effect of ADC Resolution on PES.

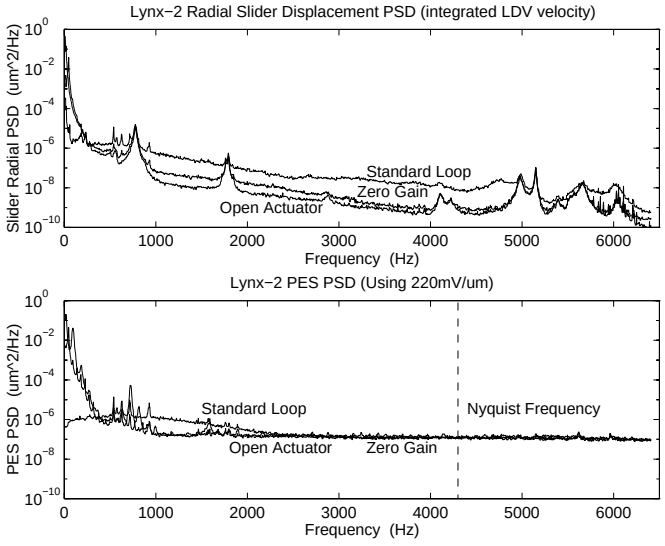

Figure 7: Radial Slider and PES Spectra vs. Loop Gain.

3.2 Slider and PES Spectra. Figure 7 illustrates the effect of loop gain on the spectra of PES and radial slider displacement. PES and LDV velocity were measured with (1) standard loop gain, (2) loop gain programmatically set to zero, and (3) the actuator physically disconnected from the servo system. In addition to the elimination of spectral lines mentioned previously, the presence of a LDV setup resonance (approximately 700 Hz) and the known disk resonances (500–1200 Hz [3]) required further smoothing of this data when performing the PES decomposition [2].

By measuring LDV and PES spectra under these loop conditions, we were able to estimate power amplifier noise (the difference between open–actuator and zero–gain measurements) and airflow or "Windage" (open–actuator response).

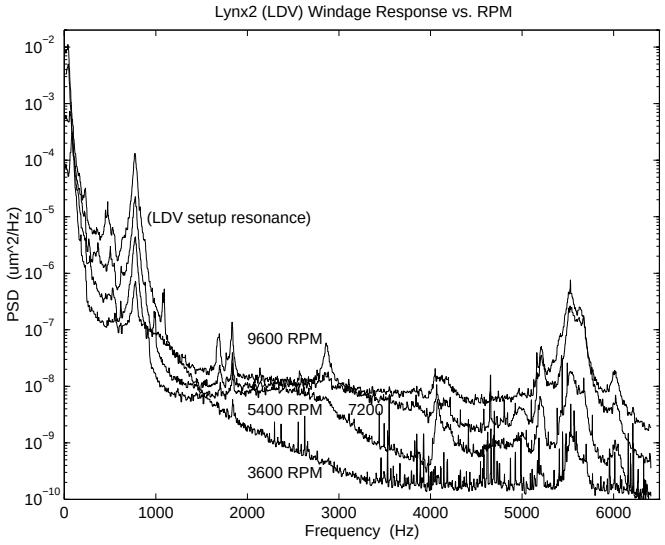

Figure 8: Radial Slider Movement vs. RPM.

Figure 8 is a series of radial slider displacement power spectra which were obtained at different rotational speeds ranging from 3600 to 9600 RPM. Again, the 700 Hz LDV setup resonance is shown (and eventually removed from the data). A series of flexure resonances are also shown between 5—6 kHz.

3.3 Position Sensing Noise. We now consider the final noise source: Position Sensing Noise (PSN). This represents the error resulting from the process of magnetically sensing and then demodulating position information as a function of the servowritten reference and the location of the head relative to this reference. The basic idea is to conduct a statistical two–way *analysis of variance* (ANOVA [4]) on the demodulated servo signal in order to provide an estimate of PSN.

The ANOVA technique has been applied to both continuous– and sectored–servo systems; differences in how each is handled are included below. This paper reports results for a continuous–servo case, but the method was originally developed for a sectored-servo disk drive [5].

3.3.1 ANOVA Modeling Assumptions. The purpose of using the ANOVA method is to partition statistical variations in data between meaningful sources—in this case, between error due to actual displacement and error due to PSN. In order to perform this analysis, we assume zero displacement across a set of n servo bits during a single servo burst observation. This seems plausible, given the relatively low frequencies of mechanical motion (less than 10 kHz) and short servo data window (less than 20 microseconds). Thus, bit–to–bit variations within an observed servo burst will be assumed to be completely due to position sensing uncertainty.

The following description uses a combination of standard statistical terms and definitions, as well as assumptions which were applied to the the position sensing process in both continuous– and sectored–servo cases. Subscripts A and B apply to the sectored–servo case, and subscripts C and D refer to the continuous–servo case, for which results are reported in section 3.3.3. Where the analysis proceeds similarly, these subscripts are replaced with the general subscript Y.

Samples of size n are selected from each of k populations (each sample is from the same servo burst, observed at k different times). In the sectored–servo case, the natural value of n is the number of servo bits within a given sector; for the continuous–servo case, the number chosen is somewhat arbitrary—short enough to insure the zero–displacement assumption described above but long enough to provide statistically significant variability. In the continuous–servo case reported here, $n = 18$ and $k = 32$, yielding $18 \times 32 - 1 = 575$ statistical degrees of freedom. Values for each ensemble of n bits result from different *treatments*, which are not under our direct control, but rather, applied by the servo system as it attempts to follow track center. Treatments and measurement error are both assumed to be random and mutually independent.

The response for each servo bit can now be written as

$$y_{ij} = \mu + \delta_i + \epsilon_{ij} \tag{1}$$

y_{ij} is a value of the random variable (for each A/B/C/D bit)

$$Y_{ij} = \mu + \Delta_i + E_{ij} \ ; \ \ i = 1, 2, \ \ldots \ k, j = 1, 2 \ \ldots \ n \tag{2}$$

In our case, the right–side components of Equation 2 are μ, the mean value of PES; Δ_i, the effect due to random displacement error (the "treatment"); and E_{ij}, the effect due to measurement error. Both Δ_i and E_{ij} are assumed to be normally distributed around a zero mean. The variance of Δ_i is σ^2_Δ, and the variance of E_{ij} is σ^2_Y.

The expected mean square value of treatments (displacement) and measurement error are given, respectively, by

$$E(SSD)_Y = \sigma_Y^2 + n\sigma_\Delta^2 \; ; \quad E(SSE)_Y = \sigma_Y^2 \tag{3}$$

where

$$SSD = n\sum_{i=1}^{k}(\bar{Y}_{i\cdot} - \bar{Y}_{\cdot\cdot})^2 \; ; \quad SSE = \sum_{i=1}^{k}\sum_{j=1}^{n}(Y_{ij} - \bar{Y}_{i\cdot})^2 \tag{4}$$

Here, a dot in the subscript denotes averaging across either k rows or n columns (or both, in the case of $\bar{Y}_{\cdot\cdot}$).

Estimates of σ_Δ^2 and σ_Y^2 are computed by dividing SSD and SSE by the appropriate number of degrees of freedom:

$$\sigma_\Delta^2 = \frac{SSD}{(k-1)} \; ; \quad \sigma_Y^2 = \frac{SSE}{k(n-1)} \tag{5}$$

Finally, the variance of PSN, σ_s^2, depends on how the individual servo bits are processed, which is different for sectored– and continuous–servo cases. Again, relying on the independence assumption, the sectored-servo PSN variance will be given based on a pair–wise subtraction, $Y_A - Y_B$, i.e.,

$$\sigma_s^2 = \frac{\sigma_A^2}{n} + \frac{\sigma_B^2}{n} \quad (sectored) \tag{6}$$

For the continuous–servo case, σ_s is computed in the following manner:

- Digitize several samples (at least 30) of the servo waveform (Figure 9 shows 4 of the 18 frames observed).
- Mathematically peak–detect the servo bit values.
- Use the ANOVA procedure outlined above to estimate the per–bit variance in position sensing, σ_Y .
- Mathematically generate a Gaussian noise time sequence $X(t)$, using σ_Y and a random number generator.
- Low-pass filter $X(t)$ by the servo demodulation filter:
  - $G(s) = \frac{10^{10}}{As^3 + Bs^2 + Cs^5 + D}$;
  - $Z(t) = lsim(\, G(s), X(t), t \,)$;

lsim is a Matlab linear system simulator routine; For the current servo system, $A = 8.61 \times 10^7$, $B = 3.95 \times 10^{-1}$, $C = 1.49 \times 10^5$, and $D = 10^{10}$. The resultant σ_s^2 of $Z(t)$ is an estimate of PSN.

3.3.2 Test Setup and Data Processing. The servo signals were accessed by connecting a HP 54720D digital oscilloscope to drive electronics via a Textronix P6046 differential probe in order to improve common mode noise rejection. Data acquisition was triggered using the drive's once–around index pulse. The number of instantaneous runs taken was 32 (each having 3278 data points). An ASCII file was produced for each of the 32 runs and transferred to the Matlab environment to compute the peak–detect C– and D–bit values for each set of 18 servo frames. The result was a 18–by–32 array of values for ANOVA use.

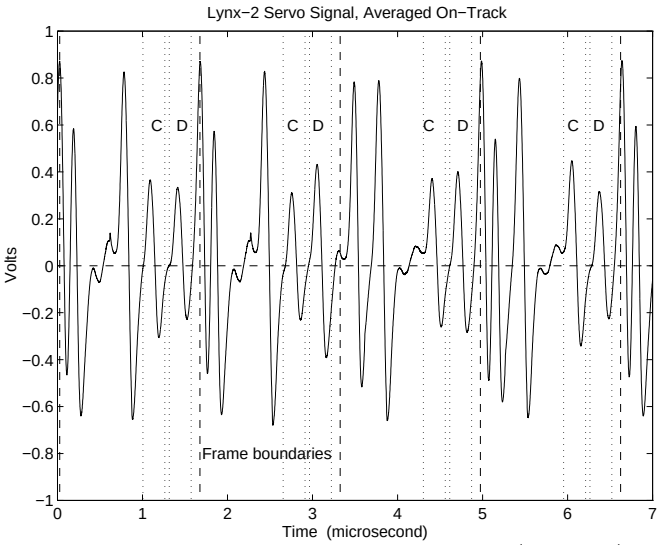

Figure 9: Four–frame sample of servo signal (averaged).

3.3.3 Test Results The ANOVA summary for our continuous–servo case is presented in Table 1. The bit variances are given by $\sigma_C^2 = 0.264\ \mu m^2$ and $\sigma_D^2 = 0.275\ \mu m^2$. So, a mid–range value of $0.269\ \mu m^2$ is used for σ_Y. This value was used to generate a random sequence $X(t)$, which was then filtered using the Matlab *lsim* routine. Histograms of the sensed and demodulated distributions are given in Figure 10. Thus, $\sigma_s = 0.0295$ microns. This value was shown to closely match the predicted value reported in our PES Pareto decomposition paper [2].

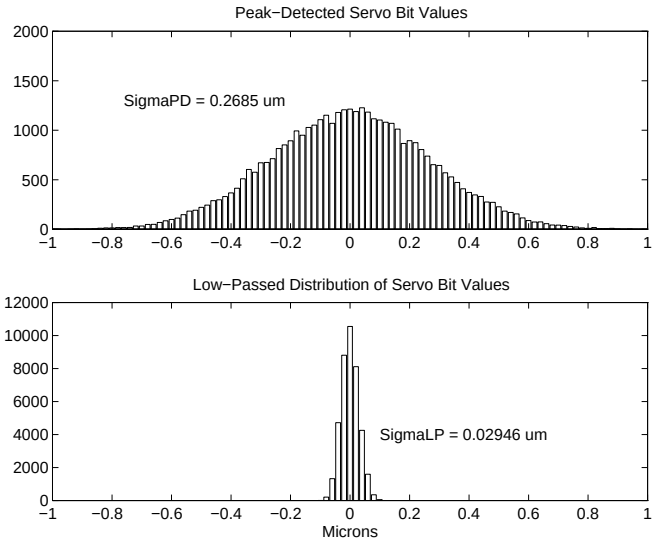

Figure 10: Measured and Filtered Position Sensing Noise.

4. Summary

The measurements described above are accomplished by connecting to test points which are typically available for all disk drive products in the normal development process. The idea is to isolate each component of the servo system by making measurements on either side—where possible—or, as the case for Position Sensing Noise, collect data and analyze it under a set of reasonable assumptions (i.e. white noise). With this data in hand, it is possible to complete the third step in the Pes Pareto

Source of Variation	C–Bits				D–Bits			
	Sum of Squares	DOF	Mean Square	Sqrt (micron)	Sum of Squares	DOF	Mean Square	Sqrt (micron)
Displacement	1.58	31	0.051	0.226	1.54	31	0.050	0.223
Meas. Error	38.05	544	0.070	0.264	41.25	544	0.076	0.275
Total	39.63	575			42.79	575		

Table 1: Analysis of Variance Estimate, Lynx-II Sensor Error.

method, namely, determining the effects of individual noise contributors on PES [2]. Thus, the collection of required data is accomplished in a fairly straightforward manner, assuming care is taken to take sufficient, high–quality measurements.

References

[1] D. Abramovitch, T. Hurst, and D. Henze, "The PES Pareto Method: Uncovering the strata of position error signals in disk drives," in *Submitted to the 1997 American Control Conference*, (Albuquerque, NM), AACC, IEEE, June 1997.

[2] D. Abramovitch, T. Hurst, and D. Henze, "Decomposition of baseline noise sources in hard disk position error signals," in *Submitted to the 1997 American Control Conference*, (Albuquerque, NM), AACC, IEEE, June 1997.

[3] J. S. McAllister, "The effect of disk platter resonances on track misregistration in 3.5 inch disk drives," *IEEE Transactions on Magnetics*, vol. 32, pp. 1762–1766, May 1996.

[4] R. E. Walpole and R. H. Myers, *Probability and Statistics for Engineers and Scientists*. New York, NY: Macmillan, second ed., 1972.

[5] T. Hurst and D. Henze, "Estimating Position Sensing Uncertainty in a Disk Drive Track–Follow System," tech. rep., Hewlett–Packard Laboratories, Palo Alto, CA, USA, October 1994.